UNIVERSITÀ DEGLI STUDI DI PADOVA

DIPARTIMENTO DI BIOLOGIA

Corso di Laurea in Biologia

UNIVERSITÀ
DEGLI STUDI
DI PADOVA

ELABORATO DI LAUREA

Exploring mitochondrial contact sites in PINK1 overexpressing cells

Tutor: Prof.ssa Marisa Brini
Dipartimento di Biologia

Laureando: Giorgio Muneretto

ANNO ACCADEMICO 2021/2022

INDEX

ABSTRACT

Membrane contact sites are regions of proximity between organelles' membranes involved in the exchange of material and information between them. They represent an important hub for the normal functioning of the cell and ultimately its health. Dysregulation in organelles function, especially mitochondria, has been found in many different neurodegenerative conditions among which Parkinson's disease (PD). Early onset autosomal recessive forms of familiar PD are linked with mutations in genes whose protein products play a key role in the process of mitochondrial quality control. Among them, the gene encoding the mitochondrial serine threonine kinase PINK1 and the one encoding the cytosolic ubiquitin ligase Parkin are the most deeply investigated. While some indirect evidence for the involvement of PINK1 in the control of contact sites between mitochondria and endoplasmatic reticulum is present in the literature, nothing is known about the possibility that it could play a role in the regulation of contact sites between mitochondria and lysosomes, which are involved in the mitophagy pathway that is disfunctional in Parkinson's disease, and even less is known about the contact sites with the nucleus. The purpose of the study presented in this thesis is to search for a causative effect of the overexpression of PINK1 on the number of contact sites between mitochondria and nucleus, mitochondria and lysosome and mitochondria and endoplasmatic reticulum membranes. A splitGFP palette of sensors (SPLICS S-P2A) developed in the laboratory was employed to monitor contact sites occurring at discrete locations. The SPLICS S-P2A method was used to count the contact sites in HeLa cells overexpressing myc-tagged PINK1 and statistical analysis allowed to assess the difference compared to the control cells that didn't overexpress PINK1. A decrease in the number of contact sites involving the endoplasmatic reticulum was found, as previously reported, a weaker decrease concerning the number of mitochondria-nucleus contacts with more difference between individual cells, and no detectable change in the number of contacts with the lysosomes. More research is needed to have a better picture of the meaning of this reorganization of the contact sites and to untangle the factors behind it.

1. Parkinson's disease

Parkinson's disease (PD) is, after Alzheimer's, the most common neurodegenerative disorder. At least 0.3% of the global population is affected, reaching 3% or more in people older than 80. There are different classifications for Parkinsonism and Parkinson's disease. Parkinson's disease identifies what is otherwise called primary or idiopathic Parkinsonism (around 80% of cases), characterized by a decrease in dopamine levels due to the loss of dopaminergic neurons in the substantia nigra pars compacta; Parkinsonism more broadly encompasses conditions with similar symptoms, like wide motor disruption, such as familiar Parkinson's, early onset Parkinson's, secondary Parkinson's, drug induced Parkinsonism (Poewe W et al, 2017).

Age is the most important risk factor; other factors associated with the risk of PD are gender (male), injection of certain substances like 1-methyl-4-phenyl tetrahydropyridine (MPTP), exposure to environmental substances like pesticides, antagonists for beta-2 adrenoreceptor, which acts by enhancing α-synuclein (α-Syn) gene SNCA (Synuclein Alpha) transcription, genetic factors. Although heritable forms of PD account for only a small percentage of incidences, around 10%, studies on these families provided insight on the genetics and the pathogenesis of the disease.

PD has been historically defined as a movement disorder, the main symptoms being speech and movement disturbances such as slowness, reduced amplitude and motion interruption, tremor, rigidity and postural instability. However non motor symptoms are an important aspect of the clinical picture, including a wide range of symptoms: fatigue, depression, sleep disorders, gastrointestinal problems, cognitive loss, sialorrhoea, reduced or absent perception of smell. The characteristic pathophysiological features of PD, definitive for the diagnosis of idiopathic PD, include neuronal loss of dopaminergic (DA) neurons in the substantia nigra pars compacta (SNpc) and progressive intracellular α-Syn accumulation (Balestrino R and Schapira AHV, 2020).

Some genes were found to be involved in PD and in 5% - 10% of cases the link was causal. Among the causal genes we find SNCA encoding α-Syn, being the first gene historically linked to PD: point mutations and multiplications of SNCA confer to α-Syn tendency to misfold and form oligomers (A53T mutation), the overexpression or reduced clearance of the protein can cause its accumulation. A-Syn accumulation, soluble as a monomer, starts with the formation of protofibrils and later insoluble fibrils that create aggregates, sometimes referred to as Lewy bodies of which α-Syn is the main component. PTEN-induced kinase 1 (PINK1, PARK6 gene) and Parkin (PARK2) interplay in a mitochondria quality-control pathway: PINK1 is a serine/threonine kinase, which activates the mitophagy pathway through the recruitment of Parkin, an E3 ubiquitin ligase. PINK1 accumulation on the OMM caused by the loss of mitochondrial membrane potential leads to parkin ubiquination and removal of dysfunctional mitochondria. Mutations of PARK2 and PARK6 are cause of PD, involving different pathways affected by mitochondrial clearance malfunctions. DJ-1 (Protein Deglycase) regulates calcium flux in the mitochondria and protects the intracellular environment from oxidative stress, functioning as an antioxidant. Knocking out or mutations of DJ1 (also known as PARK7) associated with early-onset autosomal recessive PD cause oxidative stress in the intracellular environment. LRRK2 (leucine-rich repeat serine/ threonine-protein kinase 2) mutations are associated with mitochondrial and LAS (Lysosomal Autophagy System) dysfunction and increased α-Syn aggregation in DA neurons already exposed to α-Syn fibrils. GBA (Glucosylceramidase Beta; encodes for glucocerebrosidase, a lysosomal enzyme that metabolizes glucosylceramide) mutations are associated to LAS dysfunction and α-Syn aggregation. LRP10 (LDL Receptor Related Protein 10; a protein that shuttles between the trans-Golgi, endosomes and plasma membrane)

mutations among its roles in PD also interferes with α-Syn accumulation (Chen C et al, 2019)

2. PD & Membrane Contact Sites (MCSs)

MCSs are dynamic regions of close apposition between membranes of organelles that mediate multiple functions. Among such functions are autophagy, calcium and lipid signaling, membrane dynamics, protein and lipid metabolism, cellular stress responses and energy homeostasis. The most studied interactions happen between the ER and other organelles such as mitochondria, PM, Golgi, peroxisomes and LD, but are also found between other organelle pairs, predominantly concerning mitochondria (Rossini M et al, 2020). The distance between membranes is usually between 10 nm and 50 nm but in some cases, it can reach up to 300 nm. Fundamental components of MCSs are tethers, specialized proteins that maintain the contact, forming complexes or interacting with membrane lipids.
It has been shown that altered mitochondrial – organelle communication at contact sites is a feature of the pathogenesis of PD (Ray B et al, 2021). The most studied dysfunctional interactions involve the endoplasmatic reticulum (ER) at MERCSs (Mitochondria-ER contact sites); other organelles are lysosomes and the nucleus.

2.1. Lysosomes – Mitochondria Communication

The best studied connection between lysosomes and mitochondria is related to the role of lysosomes in the degradation of mitochondria (mitophagy). Mitochondria which are considered damaged and thus must be eliminated go through mitophagy and autolysosome formation. Mitochondrial derived vesicles (MDVs) released from the mitochondria in response to mitochondrial damage are directly targeted for digestion to lysosomes. These processes maintain functional organelles within the cell preventing a potentially damaging production of ROS. Beyond the degradative connection between the two organelles, their communication is also involved in their normal functioning. If the mitochondrial normal function is disrupted, lysosomal function is found to be impaired; the transcription factor EB (TFEB) regulates lysosomal biogenesis and autophagy and it has been found to regulate mitochondrial biogenesis as well, suggesting a strong connection between these two organelles. Interestingly, an increases in the lysosomal pH value due to the inhibition of the vacuolar-type H-ATPase causes a reduction in the basal and maximal mitochondrial oxygen consumption rates (OCR), further sustaining an intimate relationship between the mantainement of mitochondrial and lysosomal function.
There is no information in the literature about possible defective lysosome-mitochondria communication in Parkinson disease but it is instead evident that many PD-related proteins have an established role in maintaining both lysosomal and mitochondrial functionality.
Vacuolar protein sorting-associated protein 35 (Vps35) is involved in autophagy and binds other proteins to form the retromer, a trimeric cargo-protein complex that transports proteins between structures such as endosomes, lysosomes and the Golgi. Mitofusins (Mfn1 and Mfn2) are proteins responsible for the fusion of the

outer mitochondrial membrane (OMM); dynamin-like protein 1 (DLP1) associates with mitochondria and functions as an OMM fission protein; the multifunctional mitochondrial E3 ubiquitin ligase 1 (MUL1) is present on the OMM and regulates mitochondrial morphology and has proapoptotic functions. VPS35 stabilizes MFN2 and induces the degradation of MUL1, supporting mitochondrial fusion. VPS35 deficiency or mutation interfere with the degradation of MUL1 and consequently impede mitochondrial fusion. Moreover, an increased direct interaction between DLP1 and the VPS35 mutant, observed also under oxidative stress conditions, interferes with mitochondrial dynamics. Heterozygous mice for VPS35 at 12 months old presented loss of DA neurons and α-Syn accumulation. Flies heterozygous for both VPS35 and parkin showed DA neuronal loss and enhanced susceptibility to the PD linked toxin paraquat. Vps35 overexpression in parkin-mutant fly models rescued many of the phenotypes, but the same was not true for PINK1-mutant flies (Plotegher and Duchen MR, 2017).
Accumulation of α-Syn is responsible for defective mitophagy and malfunctional mitochondria (Nakamura K et al, 2011). Leucine-rich repeat kinase 2 (LRRK2) is a protein involved present in the citosol or associated with the OMM and it can interact with parkin. LRRK2 has a role in different pathways such as autophagosome formation, mitochondrial function, maturation of lysosomes and vesicle trafficking. LRRK2 mutations are not rare, with a point mutation in G2019S responsible for up to 40% genetic cases of PD, and they alter mitochondrial dynamics through direct interaction with DLP1. Moreover, LRRK2 mutations reduce membrane potential and cause uncoupling of mitochondrial oxidative phosphorylation through increase in uncoupling protein (UCP) expression. It is unclear, in α-Syn and LRRK2 associated PD, if the damage starts in the mitochondria or the lysosomes and how it spreads; it's possible that the mitochondria and autophagic-lysosomal pathways are simultaneously impaired before affecting each other in any meaningful way (Plotegher N and Duchen MR, 2017); an interesting hypothesis is that the exchange of signals through the contact sites between the membranes is the way for them to communicate with each other.
Mutations in PARK2 is the most frequent cause of autosomal recessive early-onset PD followed by PARK6 mutations. Their main function is the clearance of dysfunctional mitochondria through ubiquitination and subsequent degradation in lysosomes; excess of damaged mitochondria through PARK2 or PARK6 mutations leads to oxidative stress which in turn impairs lysosomal degradation. Other than their role in mitochondrial quality check, loss of function PARK2 in PD patient fibroblasts leads to dysfunctional retromer and loss of function PARK6 inhibits lysosomal function (Demers-Lamarche J et al, 2016).

2.2. Nucleus – Mitochondria Communication

Nucleus and mitochondria communication is fundamental for the normal activity of both organelles and occurs in both directions: the anterograde pathway goes in the direction nucleus vs. MT and the retrograde pathway in the opposite one from mitochondria to the nucleus. In the anterograde pathway, around 99% of mitochondrial proteins are encoded by nuclear genes, among them the most abundant are proteins needed in mitochondrial biogenesis and all the all factors that regulate mitochondrial DNA transcription and translation. On the other hand, in the retrograde pathway, the mitochondria modulate nuclear gene expression,

cellular protein activity and in response to mitochondrial stress or dysfunction, mitochondrial production of mitokines promotes the communication with the nucleus and activates nuclear response in terms of transcription.
NRF1 induces the degradation of dysfunctional mitochondria by increasing the expression of PARK2 and PARK6 in DA cell SH-SY5Y (Lu Y et al, 2020). P62, also known as SQSTM1 (sequestosome 1), is a protein that anchors the autophagosome to ubiquinated proteins for degradation. NRF2 is involved in the parkin/PINK1 pathway by positively regulating the expression of p62. Loss of function of SQSTM1 induces α-Syn accumulation which in turn could be responsible for PD pathogenesis.

2.3. Endoplasmatic Reticulum – Mitochondria Contact Sites

ER membrane portions called mitochondria-associated membranes (MAMs) form contact sites with up to 20% of the OMM at distances in the range 15 to 50 nm. This association constitutes a key signaling hub to regulate several fundamental cellular processes including lipid metabolism, inflammation, Ca^{2+} signaling, cell survival, autophagy, intracellular motility of both organelles, and protein homeostasis (Lin TK et al, 2020). Because of the variety of the roles taken by mitochondrial endoplasmatic reticulum contact sites (MERCSs), their dysfunction may be involved in Ca^{2+} dysregulation, defects in axonal transport, neuroinflammation, loss of cellular proteostasis and mitochondrial dysfunction found in PD.
Ca^{2+} signaling is the most studied inter-organelle communication pathway and the contact sites between ER and MT are those where this communication mainly occurs. The major site of Ca^{2+} storage in the cell is the ER, where Ca^{2+} ions reach an intraluminal concentration similar to that in the extracellular ambient, i.e. around 1 mM, ten thousand fold higher than that in the cytoplasm under resting conditions(100nM), although it may be different according to the different regions of the ER and cell types. Ca2+ release from the ER to the cytosol generally occurs following a stimulus that induces the generation of a second messenger, the inositol 1,4,5 triphosphate (IP3), and the opening of IP3 sensitive Ca^{2+} channels located on the ER membrane. Ca^{2+} release from the endoplasmatic reticulum is accompanied by the uptake by the mitochondria through the mitochondrial calcium uniporter (MCU) and the concomitant opening of Ca^{2+} channel on the plasma membrane that mediate Ca^{2+} influx from the extracellular ambient to replenish the depleted ER. Signaling between ER, mitochondria and plasma membrane as well requires close apposition of their membranes which occurs at specific contact sites, involving proteins and complexes such as the inositol 1,4,5 triphosphate receptor (IP3R)/glucose-regulated protein 75 (Grp75)/voltage dependent anion channel 1 (VDAC1) complex (IP3R3–Grp75–VDAC1) and the vesicle-associated membrane protein associated protein B (VAPB)/protein tyrosine phosphatase interacting protein 51 (PTPIP51) complex (VAPB-PTPIP51).
IP3R is the ER Ca^{2+} release channel, VDAC1 is the OMM uptake channel and Grp75 is a bridging protein that interacts with IP3R and VDAC1. ER to mitochondria Ca^{2+} transfer locates at MERCSs and uses the IP3R3–Grp75–VDAC1 complex which, together with the MCU, is called the intracellular calcium regulation axis. The Ca^{2+} released from the ER accumulates between the

ER and the mitochondria, enters the mitochondrial intermembrane space and then crosses the IMM via the MCU. Dysfunction in MAMs alters the IP3R-GRP75-VDAC1 complex, mitochondrial Ca^{2+} homeostasis and leads to mitochondrial dysfunction and causes DA cells death in PD (Ray B et al, 2021). DJ1, a PD related protein, interacts with the IP3R3–Grp75–VDAC1 complex (Basso V et al, 2020); loss of function of PARK7 reduces the stability of the IP3R3–Grp75–VDAC1 complex thus inducing reduced MERCSs formation and dysfunctional mitochondria in neuronal cells and *in vivo*, forming a causative factor for PD. Mutant α-Syn tends to localize at MAM (Guardia-Laguarta C et al, 2014) and promote ER mitochondria tethering (Calì T et al, 2012); α-Syn binds to VAPB and the overexpression of its either wildtype or familial mutant form causes its accumulation at the MAM and disruption of the VAPB-PTPIP51 complex therefore interfering with its roles: decreased ER–mitochondria communication, impaired Ca^{2+} homeostasis, induced mitochondrial fragmentation and autophagy (Calı` T et al, 2019, Pailusson S et al, 2017). The VAPB–PTPIP51 complex, formed by integral ER protein VAPB and MOM localized PTPIP51, works as a tether at MERCS thus regulating autophagy and affecting Ca^{2+} transfer. It has been found to regulate synaptic functions where it localizes; mutation of its components can cause damage to ER-mitochondria signaling and contribute to synaptic dysfunction.

PINK1 and parkin localize at MERCs and the mitophagy pathway that depends on them is involved in disturbed Ca^{2+} transferring, mitochondrial fragmentation, trapped mitochondrial movement, loosening ER/mitochondrial contact, recruitment of autophagic machinery to dysfunctional mitochondria, and acquirement of membrane components from the ER for autophagosome membrane formation (Lin TK et al, 2020). At damaged mitochondria, the proautophagic protein Beclin1 relocalizes at the locations of MERCSs where the autophagosome originates, inducing its formation. PINK1 silencing impairs the recruitment of Beclin1 at MERCs and consequently the mitophagical process. Mfn2 functions as a tether at MERCS and it is ubiquitinated by parkin/PINK1 and subsequently disassembled to permit mitochondrial fission and destruction of MERCS; this process is disrupted or accelerated in case of alterations of the parkin/PINK1 pathway. Parkin is also involved in Ca^{2+} homeostasis, which is disrupted when parkin accumulates at MERCS caused by its overexpression (Cali T et al, 2013). Protein kinase R (PKR)-like endoplasmic reticulum kinase (PERK), induced by misfolded proteins-ER stress, is an enzyme that leads to the inactivation of the eukaryotic Initiation Factor 2 (eIF2) necessary for most translation initiations. In Drosophila models of PD, parkin and PINK1 mutations induce neurotoxic ER stress through activation of PERK.

3. Study of Contact Sites

The study of contact sites can be approached using different methods, which have been tested with special focus on the most studied ER-mitochondria contact sites. In situ proximity ligation assay (PLA) is a technique used to visualize proteins that are in proximity, closer than 40 nm, or part of a protein complex. Two primary antibodies from different species recognize specific antigens of the proteins of interest. Secondary antibodies, also called PLA probes, bind to the primary antibodies, and are attached to a short DNA strand. Adding specific DNA

oligonucleotides, substrates and enzymes, the proximity of the proteins enables the DNA strands to participate in rolling circle replication (RCR). After the DNA is amplified, fluorescent-labeled complementary oligonucleotide strands are added, and the proteins can be viewed under a fluorescence microscope. PLA has its limitations, namely: it can only be used in fixed cells and is limited by the availability and the specificity of the antibodies. High resolution imaging can be achieved using electron microscopy (EM) but it can only be used on fixed samples and the analysis of a consistent number of images corresponding to different cellular sections/planes is very time consuming. The use of fluorescent proteins (FPs) is another commonly used method, offering the advantage to visualize contact sites in living cells upon their illumination under confocal microscope. The fluorescent proteins in question can be easily targeted the membrane of the organelle of interest by adding to their sequence specific localization signals, i.e. the first application of this approach was employed to reveal ER and mitochondria proximity (Rizzuto et al, 1998). The drawbacks of this approach are the limited resolution in the distance range below 200 nm, the eventual differences in FPs expression levels and possible alterations in organelle morphology due to the overexpression of exogenous fluorescent proteins on the surface. To overcome these limits, two FP-based sensors of proximity were developed: a dimerization-dependent FP (ddFP) or Venus FP and a FRET-based probe coupled to a rapamycin-binding module (FEMP). They allowed to improve the study of contact sites at shorter distances, however the ddFP probe is intrinsically not extremely bright and the FRET probe requires equimolar expression of the two moieties. In addition, its applications *in vivo* are limited by the requirement of rapamycin application to the cells, a potent inducer of autophagy, to maximize membranes juxtaposition and FRET signal. Another issue is related to the fixed distance at which they work which is based on the linker and it's not flexible.

To find a solution to the problems above and to develop a sensor applicable also for *in vivo* studies, a new approach based on the splitGFP and Bimolecular fluorescent complementation (BiFC) technique was applied to generate split contact site sensor (SPLICS). SPLICS is a one-step imaging technique that has been initially generated to identify narrow and wide ER–mitochondria apposition that occurs in a different range of distance, i.e. between 10 and 50 nm. In particular two types of sensors were developed to respectively monitor contact sites occurring at 8-10nm distance and at 40-50nm distance. The sensor consists of a single vector containing two split GFP moieties, the Beta 11 portion and the GFP 1-10 fragment, which have lost their properties to emit fluorescence. Each of these portions can be fused with a specific localization sequence that targets them to a precise location/organelle into the cell. Only when the two fragments of the split-GFP colocalize and are close enough to permit the complementation process, the two moieties can reconstitute the original green fluorescence of the whole GFP protein (Cieri D et al, 2018).

4. Purpose of Study

PINK1 is a mitochondrial serine threonine kinase whose mutations are linked to the development of familiar Parkinson's disease. It is implicated in the process of mitochondrial quality control, i.e. mitophagy where dysfunctional mitochondria

are engulfed in autophagosome and are degraded upon fusion with the lysosome. PINK1 is also involved in the apoptosis and in the mitochondria shape remodeling. Overexpression of PINK1 promotes mitochondrial fission while its downregulation promotes mitochondrial fusion and both events require activity at contact sites with other organelles, among which ER and lysosomes are best known to be involved. The possibility that PINK1 could play a direct role in the modulation of organelles contact sites has not been investigated. The aim of this study is to clarify this aspect by directly monitoring contact sites in cells overexpressing PINK1.

5. Materials & Methods

5.1 Plasmid

SPLICS S-P2A Nu-MT, SPLICS S-P2A ER-MT, and SPLICS S-P2A Ly-MT were designed and obtained by custom gene synthesis (Thermo Fisher Scientific). The ER-, nucleus- and lysosome-targeting sequence were fused with a short linker (10nm) and the β-sheet 11 moiety of the SPLICS system, while the MT-targeting sequence was fused with the GFP1.10 moiety. To ensure an equimolar expression the β-sheet 11 moiety was inserted upstream of a self-cleaving viral 2A peptide (P2A) followed by the GFP1.10 part. PINK1 was myc-tagged. PcDNA3 was used as an empty vector.

5.2 Cell Cultures

HeLa ATTC cells were used, kept at 37°C in a 5% CO2 atmosphere in Dulbecco's modified Eagle's medium (DMEM) high glucose (Gibco; 41966-029). DMEM was complemented with 10% Fetal Bovine Serum (FBS) (Gibco; 10270-106), 100 U/ml penicillin and 100 mg/ml streptomycin (Penicillin–Streptomycin solution 100X) (EuroClone; ECB3001D).

5.3 Transfection

HeLa cells were seeded at 60–80% confluence on 13mm diameter glass coverslips. Twenty hours later they were transfected through the Ca^{2+} phosphate protocol, where the plasmids were mixed with a concentrated solution of CaCl2 and then added to a phosphate buffer forming a precipitate. The co-transfection used in a 1:1 ratio on one hand the SPLICS short GFP Lysosome-Mitochondria (SPLICS S Ly-MT), short GFP Nucleus-Mitochondria (SPLICS S Nc-MT) and short GFP Endoplasmatic Reticulum-Mitochondria (SPLICS S ER-MT) and on the other WT PINK1 fragments respectively. Control cells were transfected under the same conditions, with an empty vector and the probes without PINK1.

5.4 Immunocytochemistry

24 hours after the transfection the plated cells were fixed with 3.7% formaldehyde (Formaldehyde stock solution 37% in H2O) (Sigma-Aldrich; F8775) in Phosphate

Buffered Saline (PBS) (EuroClone; ECB4004L) for 20 min and washed three times with PBS. The cells were then permeabilized for the primary antibody, undergoing 20 min incubation in 0.1% Triton X-100 Bio-Chemica (PanReac AppliChem; A1388) in PBS, followed by two washes in 1% gelatin/PBS (Type B from bovine skin) (Sigma-Aldrich; G9382) for 15 min and washing in PBS at room temperature (RT) for 15 min. The coverslips were then incubated for 90 min at 37°C or RT with the specific primary antibody diluted in PBS (anti-TOM20, mouse, Santa Cruz Biotechnology, SC-17764; anti-TOM20, rabbit, Santa Cruz Biotechnology, SC-11415; anti-c-myc, Sigma-Aldrich, C-3956; anti-c-myc, Roche, 11667149001). The excess of primary antibody was removed through washing with gelatin and PBS following the steps mentioned above. Alexa Fluor secondary antibodies (Thermo Fisher: anti-Mouse IgG Alexa Fluor 405, goat, A-31553; anti-Rabbit IgG Alexa Fluor 594, A-11012; anti-Rabbit IgG Alexa Fluor 647, donkey, A-32795; anti-Rabbit IgG Alexa Fluor 568, goat, A-11036) were then applied, the cells incubated for 45min at room temperature and then washed with PBS to remove secondary antibody excess. Mowiol 40-88 (Sigma-Aldrich; 81386) was used to mount the coverslips.

5.5 Confocal microscope analysis

Cells were observed 24 h after transfection with a ZEISS LSM900 Airyscan2 confocal microscope, using a Plan-Apochromat 63X/numerical aperture 1.40 oil immersion DIC M27. The images were acquired upon excitation with lasers at the wavelength of 405, 488, 568, 594 and 647 nm. Z-stack of the cells were acquired every 0.29µm, then processed using ImageJ. To count different types of dots, images were first convolved, and the cells were selected by freehand selection of ImageJ in the drawing/selection polygon tool and then processed using the "Quantification 1" plug-in (https://github.com/titocali1/Quantification-Plugins). A 3D reconstruction of the resulting image was obtained using the VolumeJ plug-in (https://github.com/titocali1/Quantification-Plugins). A selected face of the 3D rendering was then thresholded and used to count short and long contact sites through the "Quantification 2" plug-in (https://github.com/titocali1/Quantification-Plugins).

5.6 Statistical analysis

Results are reported as means ± SEM and Gaussian distribution was assessed by D'Agostino-Pearson omnibus and Shapiro-Wilk normality tests. Statistical analysis of two groups was obtained applying unpaired Student's two-tailed t test (Gaussian distribution) or Mann-Whitney test (no-Gaussian distribution). To compare more of two groups one-way/two-way ANOVA test (Gaussian distribution) or Kruskal-Wallis test (no-Gaussian distribution) was used. Significance was fixed at $p \leq 0.05$ and calculated using GraphPad Prism 8

(GraphPad, San Diego, CA, USA). In figures legend, n= number of at analyzed cells from at least three independent transfections.

6. Results and Discussion

SPLICS S (Short)-P2A was used to assess the contact sites between mitochondria and nucleus, lysosome and endoplasmatic reticulum; at the same time overexpression of myc-tagged PINK1 was analyzed in the context of the contact sites, using an empty vector and probe without PINK1 as control. The Short SPLICS sensors allow the study of interactions happening in the range of 8-10nm; the SPLICS S-P2A have a P2A peptide inserted between the beta 11 moiety and the GFP 1-10 one, which allows for an equimolar expression of the fragments. 36 hours after transfection through the Ca^{2+} phosphate protocol using a 1:1 ratio of SPLICS and of PINK1 plasmids, the HeLa cells were fixed and incubated with primary and secondary antibodies to be observed under a confocal microscope. This made it possible to count the occurrences of contact sites, where the GFP signal was visible, while visualizing the morphology of the organelles involved and the distribution of PINK1.

6.1 PINK1 overexpression does not affect lysosome-mitochondria contact sites

To assess mitochondria-lysosome contact sites, HeLa cells were plated on coverslips and transfected with SPLICS S-P2A Ly-MT expression vector alone or together with the PINK1 plasmid. The co expression was verified by performing an immunocytochemistry analysis where PINK1 abundance was verified by incubating the cells' monolayer with an antibody that recognizes the myc-tag fused to its N-terminal region. Mitochondrial distribution of PINK1 is appreciated by the punctuate distribution of the red fluorescence signal. Mitochondria were labeled by the incubation with a primary antibody which recognizes the endogenous outer mitochondrial membrane protein TOM20, their signal is shown in blue. Lysosomal distribution was not revealed. Panels A and E show the SPLICS S-P2A signal in green, where the fluorescence results from the complementation of the beta 11-strand targeted to the lysosomes and the GFP 1-10 moiety targeted to the mitochondria. The green signal was obtained upon excitation at 488 nm and acquiring the emission of GFP fluorescence at 509nm. Panels B and F show the mitochondria in blue, where anti-TOM20 SC was used as a primary antibody and Alexa Fluor 405, with excitation spectrum at around 401nm and emission spectrum at around 421nm, was used as a secondary antibody. Panel G shows overexpressed PINK1 (which is absent in the Control as shown in Panel C) revealed in red. Panel D and H are the merging of the images in Panels A, B and C or E F and G, respectively.

Panel H clearly shows that PINK1 signal does not overlap with the green signal from the Ly-MT contact sites, suggesting that PINK1 is not directly involved in

the tethering of these two organelles. No statistical difference was seen in the mean number of contact sites between the controls and the PINK1 OE cells. This suggests that the overexpression of PINK1 doesn't impact the number of contact sites between mitochondria and lysosomes.

Control

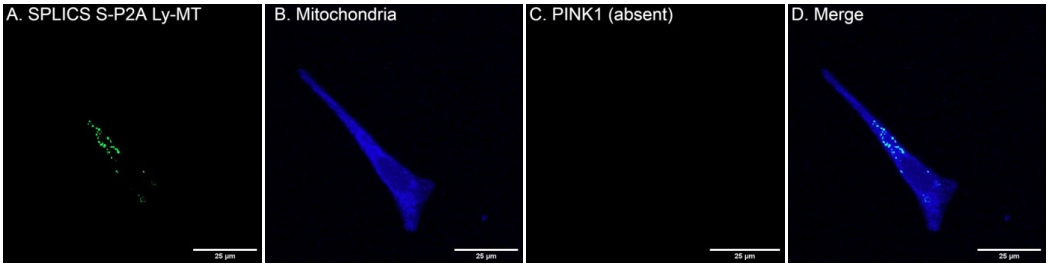

PINK1 Overexpressing cells (OE)

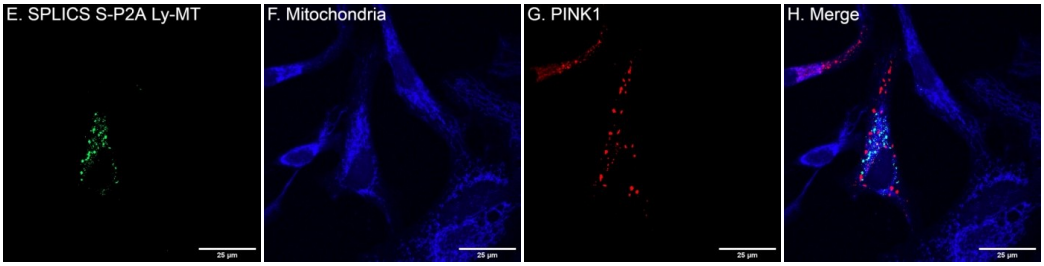

Figure 1. Z-stack projections of HeLa cells (fig. A-H). Reconstituted splitGFP fluorescence at lysosome-mitochondria contacts was shown in green, mitochondria in blue and PINK1 in red. Merge panels obtained from overlapping of the three signals. The quantification analysis was shown in Figure 2.

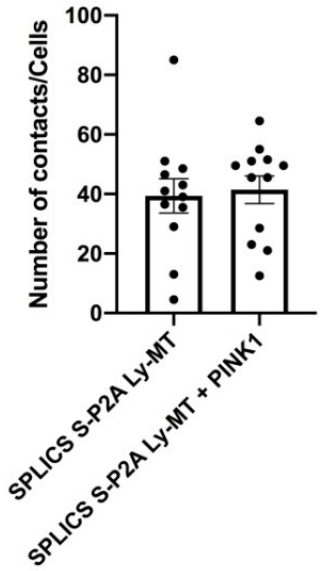

	Control	PINK1 OE
Number of analyzed cells	12	12
Mean	39.38	41.42
Std. Deviation	20.02	16.05
Std. Error of Mean	5.78	4.633

I. J.

Figure 2. Chart shows the number of contacts and their mean in Control and in PINK1 OE cells (I), and the table of the chart with the meaningful values (number of values, mean, standard deviation, standard error of mean) (J).

6.2 PINK1 overexpression shows a tendency to reduce nucleus-mitochondria contact sites in HeLa cells

To assess mitochondria-nucleus contact sites, HeLa cells were plated on coverslips and transfected with SPLICS S-P2A Nu-MT expression vector alone or together with the PINK1 plasmid. The co expression was verified by performing an immunocytochemistry analysis where PINK1 abundance was verified by incubating the cells monolayer with an antibody that recognizes the myc-tag fused to its N-terminal region. Mitochondrial distribution of PINK1 is appreciated by the punctuate distribution of the magenta fluorescence signal, using Alexa Fluor 568 with excitation spectrum at around 578nm and emission spectrum at around 600nm. The mitochondria were colored in red and their signal was revealed by immunocytochemistry performed using the primary antibody against TOM20 and the secondary antibody Alexa Fluor 647 with excitation spectrum at around 652nm and an emission spectrum at around 668. The nuclei were colored with Hoechst 33342 with an excitation spectrum of around 350nm and an emission spectrum of around 460nm. SPLICS S-P2A is visualized in green in Panels A and F thanks to the reconstitution of the beta 11-strand targeted to the nucleus and the GFP 1-10 moiety targeted to the mitochondria. Panel B and G show the mitochondria in red. Panel C and H show the nuclei in blue. Panel I show PINK1 (absent in the Control, Panel D) in magenta. Panels E and J show the merge of multiple images taken at the different channels.

A tendency toward the reduction is seen in the mean number of contact sites in PINK1 OE cells with respect to control cells. The standard error of mean, which is relatively small in the controls, appears significatively larger in the PINK1 OE cells. This suggests that the overexpression of PINK 1 could impact on the number of contact sites, although further experiments are necessary to reach a statistically significant difference.

Control

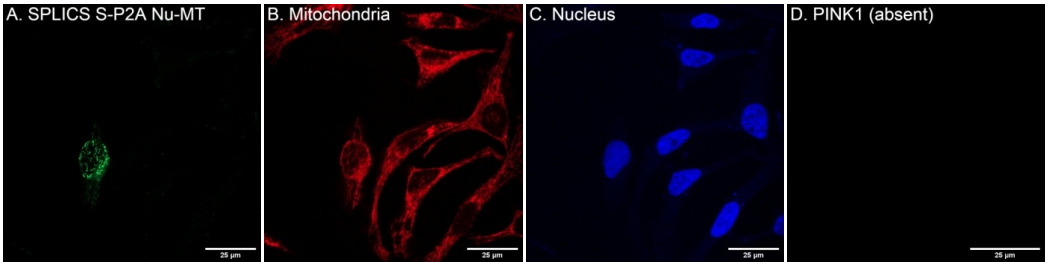

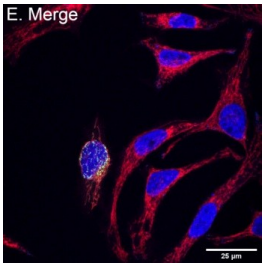

PINK1 Overexpressing cells

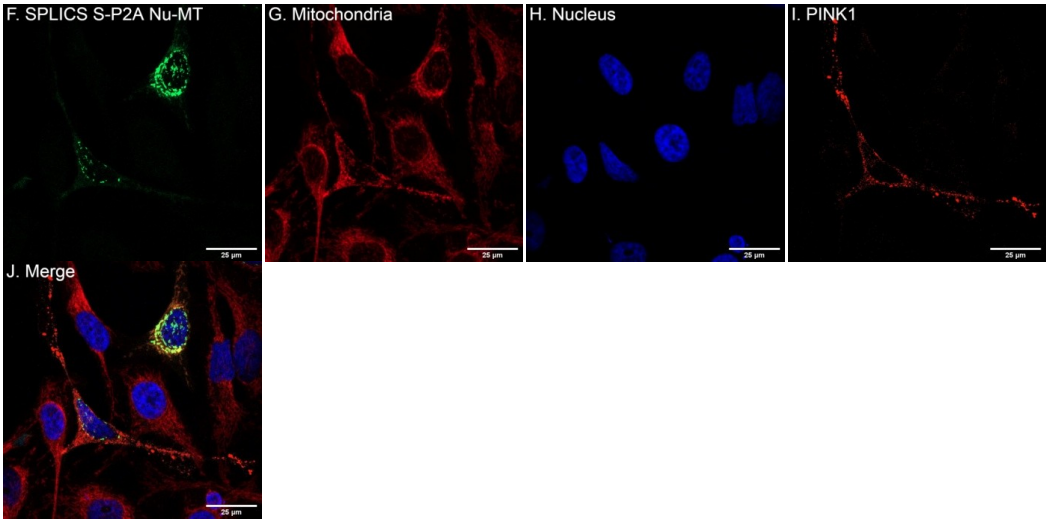

Figure 3. Z-stack projections of HeLa cells (fig. A-J). Reconstituted splitGFP fluorescence at the nucleus-mitochondria contacts was shown in green, mitochondria in red, nucleus in blue and PINK1 in magenta. Merge panels were obtained from the overlapping of the four signals. The quantification analysis was shown in Figure 4.

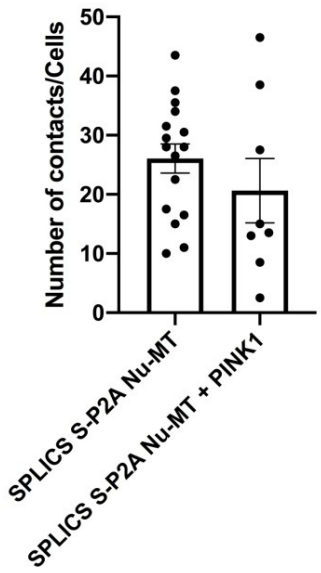

	Control	PINK1 OE
Number of analyzed cells	16	8
Mean	26.06	20.63
Std. Deviation	9.799	15.36
Std. Error of Mean	2.450	5.432

K. L.

Figure 4. Chart showing the number of contacts and their mean In Control and in PINK1 OE (K), table of the chart with the meaningful values (number of values, mean, standard deviation, standard error of mean) (L).

6.3 PINK1 overexpression significantly reduces ER-mitochondria contact sites

To assess mitochondria-ER contact sites, HeLa cells were plated on coverslips and transfected with SPLICS S-P2A ER-MT expression vector alone or together with the PINK1 plasmid. The co expression was verified by performing an immunocytochemistry analysis where PINK1 abundance was verified by incubating the cells monolayer with an antibody that recognizes the myc-tag fused to its N-terminal region. Mitochondrial distribution of PINK1 is appreciated by the punctuate distribution of the red fluorescence signal. Mitochondria were labeled by the incubation with a primary antibody which recognizes the endogenous outer mitochondrial membrane protein TOM20, their signal is shown in blue. ER distribution was not revealed. Panels A and E show the complementation of the beta 11-strand targeted to the endoplasmatic reticulum and the GFP 1-10 moiety targeted to the mitochondria of the SPLICS S-P2A reporter. In figures B and F mitochondria are revealed by the staining with Alexa Fluor 405, with excitation spectrum at around 401nm and emission spectrum at around 421nm, in blue, and anti-TOM20 was used as a primary antibody. Panel G shows PINK1 which is absent in the Control cells transected only with the SPLICs (Panel C). Figures D and H are the results of the overlapping of the images acquired in the different channels.

The merging of Panel E and G results in Panel H which shows a matching distribution of contact sites and PINK1. This is in line with the normal protein accumulation at these contact sites to modulate the crosstalk between ER and mitochondria. The mean number of contact sites of the controls appears to be more than twice as large as that of the PINK1 OE cells. This suggests that the overexpression of PINK 1 impacts on ER/mitochondria tethering by reducing it. When PINK1 doesn't translocate through the IMM-localized TIM (translocase of the inner mitochondrial membrane) 23 it accumulates in the OMM without being cleaved in the mitochondrial matrix leading to the ubiquitination of OMM resident proteins and eventually mitochondrial degradation. One of the proteins that are ubiquitinated by the parkin/PINK1 pathway is Mfn2 that forms ER-MT tethers in a homotypic complex or a heterotypic complex with Mfn1. Overexpression of PINK1 could lead to its accumulation on the OMM and to the disassembly of the tethering complex, possibly through an action on Mfn2.

Control

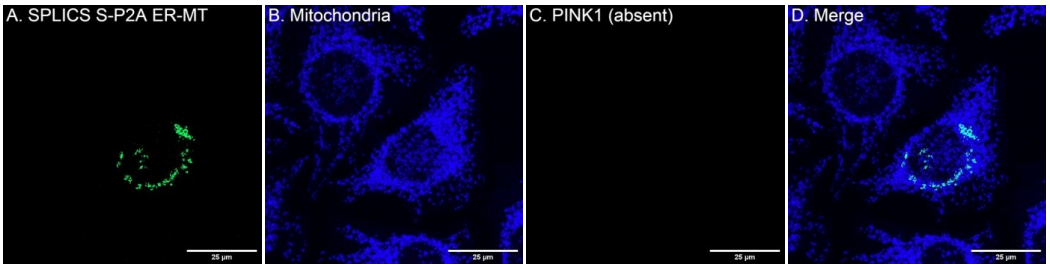

PINK1 Overexpressing cells

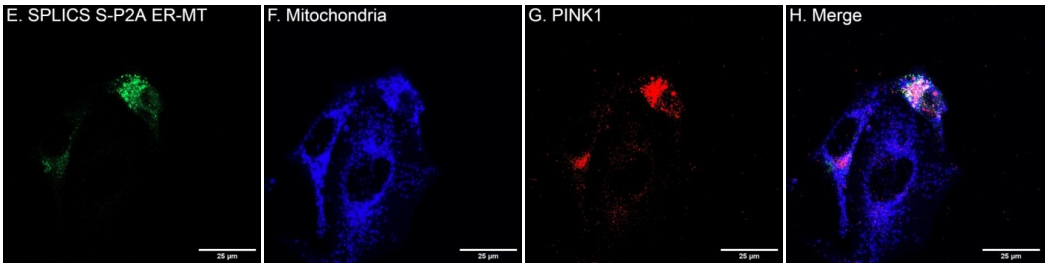

Figure 5. Z-stack projections of HeLa cells (A-H). Reconstituted splitGFP fluorescence at the ER-mitochondria contacts was shown in green, mitochondria in blue and PINK1 in red. Merge panels were obtained from the overlapping of the three signals. The quantification analysis was shown in Figure 6.

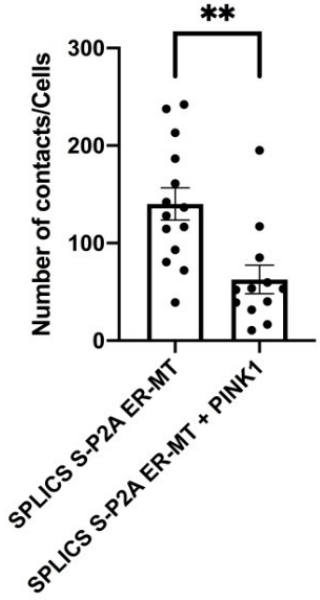

I.

	Control	PINK1 OE
Number of analyzed cells	14	12
Mean	140.1	62.71
Std. Deviation	61.88	50.60
Std. Error of Mean	16.54	14.61

J.

Figure 6. Chart showing the number of contacts and their mean In Control and in PINK1 OE (I), table of the chart with the meaningful values (number of values, mean, standard deviation, standard error of mean) (J).

6.4. Conclusions

This study has explored the effect of the Parkinson disease related protein PINK1 overexpression on mitochondria contact sites with lysosome, nucleus and endoplasmic reticulum. To this end HeLa cells were chosen as a model for overexpression. Mitochondria tethering with the other organelles was explored by the recombinant sensors SPLICS that have been generated in the laboratory where this thesis was developed. We have found that upon PINK1 overexpression the ER-MT contact sites were reduced, but the LYS-MT and the NU -MT were substantially unchanged. These findings are in line with the possibility that PINK1 overexpression could impact on mitochondrial Ca^{2+} handling. Mitochondrial Ca^{2+} overload and the resulting mitochondrial dysfunction are common elements in many neurodegenerative diseases, among which PD. PINK1 by reducing the mitochondria ER proximity could play a protective role by reducing the ER mitochondria Ca^{2+} transfer thus avoiding its excessive accumulation in the mitochondrial matrix. Loss of function mutations could be responsible for excessive Ca^{2+} accumulation and mitochondrial damage under stress conditions that are associated with increased risk to develop PD.

References

Balestrino, R. and Schapira, A.H.V. (2020) Parkinson's Disease. European Journal of Neurology, 27, 27-42. https://doi.org/10.1111/ene.14108.

Basso, V. , Marchesan, E., Ziviani, E. A trio has turned into a quartet: DJ-1 interacts with the IP3R-Grp75-VDAC complex to control ER-mitochondria interaction, Cell Calcium, Volume 87, 2020, 102186, ISSN 0143-4160, https://doi.org/10.1016/j.ceca.2020.102186.

Calì, T., Ottolini, D., Negro, A., & Brini, M. (2012). a-Synuclein controls mitochondrial calcium homeostasis by enhancing endoplasmic reticulum-mitochondria interactions. J Biol Chem, 287(22), 17914–17929. https://doi.org/ 10.1074/jbc.M111.302794.

Calì T, Ottolini D, Vicario M, Catoni C, Vallese F, Cieri D, Barazzuol L, Brini M. splitGFP Technology Reveals Dose-Dependent ER-Mitochondria Interface Modulation by α-Synuclein A53T and A30P Mutants. Cells. 2019 Sep 12;8(9):1072. doi: 10.3390/cells8091072. PMID: 31547305; PMCID: PMC6769576.

Cali, T., Ottolini, D., Negro, A., and Brini, M. (2013). Enhanced parkin levels favor ER-mitochondria crosstalk and guarantee Ca(2+) transfer to sustain cell bioenergetics. Biochim. Biophys. Acta 1832, 495–508. doi: 10.1016/j.bbadis.2013.01.004.

Cieri, D., Vicario, M., Giacomello, M. et al. SPLICS: a split green fluorescent protein-based contact site sensor for narrow and wide heterotypic organelle juxtaposition. Cell Death Differ 25, 1131–1145 (2018). https://doi.org/10.1038/s41418-017-0033-z.

Chen C, Turnbull DM, Reeve AK. Mitochondrial Dysfunction in Parkinson's Disease-Cause or Consequence? Biology (Basel). 2019 May 11;8(2):38. doi: 10.3390/biology8020038. PMID: 31083583; PMCID: PMC6627981.

Demers-Lamarche, J., Guillebaud, G., Tlili, M., Todkar, K., Bélanger, N., Grondin, M., et al. (2016). Loss of mitochondrial function impairs lysosomes. J. Biol. Chem. 291, 10263–10276. doi: 10.1074/jbc.M115.695825.

Guardia-Laguarta, C., Area-Gomez, E., Rub, C., Liu, Y., Magrane, J., Becker, D., Voos, W., Schon, E. A., & Przedborski, S. (2014). a-synuclein is localized to mitochondria-associated ER membranes. J Neurosci, 34(1), 249–259. https://doi.org/10.1523/JNEUROSCI.2507-13. 2014.

Lin T-K, Lin K-J, Lin K-L, Liou C-W, Chen S-D, Chuang Y-C, Wang P-W, Chuang J-H and Wang T-J (2020) When Friendship Turns Sour: Effective Communication Between Mitochondria and Intracellular Organelles in Parkinson's Disease. Front. Cell Dev. Biol. 8:607392. doi: 10.3389/fcell.2020.607392.

Lu, Y., Ding, W., Wang, B., Wang, L., Kan, H., Wang, X., et al. (2020). Positive regulation of human PINK1 and Parkin gene expression by nuclear respiratory factor. 1. Mitochondrion 51, 22–29. doi: 10.1016/j.mito.2019. 12.002.

Nakamura, K., Nemani, V. M., Azarbal, F., Skibinski, G., Levy, J. M., Egami, K., et al. (2011). Direct membrane association drives mitochondrial fission by the Parkinson's disease-associated protein α-synuclein. J. Biol. Chem. 286, 20710–20726. doi: 10.1074/jbc.M110.213538.

Narendra, D. P., Jin, S. M., Tanaka, A., Suen, D., Gautier, C. A., Shen, J., et al. (2010). PINK1 is selectively stabilized on impaired mitochondria to activate parkin. PLoS Biol. 8:e1000298. doi: 10.1371/journal.pbio.1000298.

Paillusson S, Gomez-Suaga P, Stoica R, Little D, Gissen P, Devine MJ, Noble W, Hanger DP, Miller CCJ. α-Synuclein binds to the ER-mitochondria tethering protein VAPB to disrupt Ca2+ homeostasis and mitochondrial ATP production. Acta Neuropathol. 2017 Jul;134(1):129-149. doi: 10.1007/s00401-017-1704-z. Epub 2017 Mar 23. PMID: 28337542; PMCID: PMC5486644.

Plotegher N and Duchen MR (2017) Crosstalk between Lysosomes and Mitochondria in Parkinson's Disease. Front. Cell Dev. Biol. 5:110. doi: 10.3389/fcell.2017.00110.

Poewe W, Seppi K, Tanner CM, Halliday GM, Brundin P, Volkmann J, Schrag AE, Lang AE. Parkinson's disease. Nat Rev Dis Primers. 2017 Mar 23;3:17013. doi: 10.1038/nrdp.2017.13. PMID: 28332488.

Ray B, Bhat A, Mahalakshmi AM, Tuladhar S, Bishir M, Mohan SK, Veeraraghavan VP, Chandra R, Essa MM, Chidambaram SB, Sakharkar MK. Mitochondrial and Organellar Crosstalk in Parkinson's Disease. ASN Neuro. 2021 Jan-Dec;13:17590914211028364. doi: 10.1177/17590914211028364. PMID: 34304614; PMCID: PMC8317254.

Rizzuto R, Pinton P, Carrington W, Fay FS, Fogarty KE, Lifshitz LM, Tuft RA, Pozzan T. Close contacts with the endoplasmic reticulum as determinants of mitochondrial Ca2+ responses. Science. 1998 Jun 12;280(5370):1763-6. doi: 10.1126/science.280.5370.1763. PMID: 9624056.

Rossini, M., Pizzo, P. and Filadi, R. (2021), Better to keep in touch: investigating inter-organelle cross-talk. FEBS J., 288: 740-755. https://doi.org/10.1111/febs.15451.

Valentina Basso, Elena Marchesan, Elena Ziviani, A trio has turned into a quartet: DJ-1 interacts with the IP3R-Grp75-VDAC complex to control ER-mitochondria interaction, Cell Calcium, Volume 87, 2020, 102186, ISSN 0143-4160, https://doi.org/10.1016/j.ceca.2020.102186.